Title	Fabrication of high-concentration Cu-doped deuterated targets for fast ignition experiments
Author(s)	Ikeda, Tomokazu; Kaneyasu, Yumi; Hosokawa, Hitomi et al.
Citation	Nuclear Fusion. 2022, 63(1), p. 016010
Version Type	VoR
URL	https://hdl.handle.net/11094/92538
rights	This article is licensed under a Creative Commons Attribution 4.0 International License.
Note	

PAPER • OPEN ACCESS

Fabrication of high-concentration Cu-doped deuterated targets for fast ignition experiments

To cite this article: Tomokazu Ikeda *et al* 2023 *Nucl. Fusion* **63** 016010

View the article online for updates and enhancements.

Fabrication of high-concentration Cu-doped deuterated targets for fast ignition experiments

Tomokazu Ikeda[1]**, Yumi Kaneyasu**[1]**, Hitomi Hosokawa**[1]**,
Keisuke Shigemori**[1]**, Takayoshi Norimastu**[1]**,
Marilou Cadatal-Raduban**[1,2]**, Keiji Nagai**[1,3,4]**, Sadaoki Kojima**[5]**,
Yuki Abe**[6]**, Eisuke Miura**[7]**, Yoneyoshi Kitagawa**[8]**, Mao Takemura**[1]**,
Yubo Wang**[1]**, Jinyuan Dun**[1]**, Shuwang Guo**[1]**, Shoui Asano**[1]**,
Ryunosuke Takizawa**[1]**, Shinsuke Fujioka**[1]**, Hiroyuki Shiraga**[1]**,
Yasunobu Arikawa**[1]**, Tetsuo Ozaki**[9]**, Akifumi Iwamoto**[9]**, Hitoshi Sakagami**[9]**,
Hiroshi Sawada**[10]**, Yoshitaka Mori**[8]** and Kohei Yamanoi**[1,*]

[1] Institute of Laser Engineering, Osaka University, 2-6 Yamada-oka, Suita, Osaka 565-0871, Japan
[2] Centre for Theoretical Chemistry and Physics, School of Natural and Computational Sciences, Massey University, Auckland, 0632, New Zealand
[3] Institute of Innovative Research (IIR), Tokyo Institute of Technology, Suzukake-dai, Midori-ku, Yokohama, Kanagawa 226-8503, Japan
[4] Frontier Science and Social Co-Creation Initiative (FSSI), Kanazawa University, Kakuma-cho, Kanazawa, Ishikawa 920-1192, Japan
[5] Kansai Photon Science Institute, Quantum Beam Science Directorate, National Institutes for Quantum and Radiological Science and Technology, 8-1-7 Umemidai, Kizugawa, Kyoto 619-0215, Japan
[6] Graduate School of Engineering, Osaka University, Suita 565-0871, Japan
[7] National Institute of Advanced Industrial Science and Technology (AIST), Tsukuba Central 2, 1-1-1 Umezono, Tsukuba, Ibaraki 305-8568, Japan
[8] The Graduate School for the Creation of New Photonics Industries, Hamamatsu, Shizuoka, 431-1202, Japan
[9] National Institute for Fusion Sciences, Toki, GIFU 509-5292, Japan
[10] Department of Physics, University of Nevada Reno, Reno, Nevada 98557, United States of America

E-mail: yamanoi-k@ile.osaka-u.ac.jp

Abstract

In high-energy-density physics, including inertial fusion energy using high-power lasers, doping tracer atoms and deuteration of target materials play an important role in diagnosis. For example, a low-concentration Cu dopant acts as an x-ray source for electron temperature detection while a deuterium dopant acts as a neutron source for fusion reaction detection. However, the simultaneous achievement of Cu doping, a deuterated polymer, mechanical toughness and chemical robustness during the fabrication process is not so simple. In this study, we report the successful fabrication of a Cu-doped deuterated target. The obtained samples were characterized by inductively coupled plasma optical emission spectrometry, differential scanning calorimetry and Fourier transform infrared spectroscopy. Simultaneous measurements of Cu K-shell x-ray emission and beam fusion neutrons were demonstrated using a petawatt laser at Osaka University.

* Author to whom any correspondence should be addressed.

1. Introduction

Fast ignition (FI) is an advanced concept in inertial confinement fusion to realize inertial fusion energy (IFE), which can optimize fuel implosion and heating processes to achieve high gain [1, 2]. In FI, understanding the mechanisms of energy transfer from fast electrons to the compressed plasma core is critical for efficient fusion fuel heating. In various experiments [3–15] characteristic x-rays produced by the laser-accelerated fast electrons were utilized to understand the mechanisms of electron transport in dense plasma, and neutrons generated during IFE experiments have been utilized to investigate the fusion reaction as well as the temperature of the compressed core. Characteristic x-rays and neutrons are measured using fuel targets containing tracer atoms that generate a specific signal during a fusion reaction in IFE experiments. The amount of tracer is important to avoid resonant self-absorption of the x-rays. The deuterated ratio of target materials is also important for an efficient fusion reaction [16]. For these purposes several targets have been developed, for example targets with a high deuterium concentration, metal foams and low-Z materials with transparency [17–19]. The type of tracer atom contained in the target depends on the purpose of the experiment.

Copper (Cu) K-shell x-ray emission has been used to visualize the distribution of energy deposition of the fast electron beam in FI experiments [13–15, 20, 21]. For this purpose, copper (II) oleate [$Cu(C_{18}H_{33}O_2)_2$, Cu-oleate] microsphere targets are fabricated with Cu contents of 9.7 wt% [11]. In addition, deuterated polystyrene targets [22] can generate neutrons during IFE experiments; these allow investigation of the fusion reaction as well as the temperature of the compressed core. Cu-oleate and deuterated polystyrene microsphere targets are usually fabricated by the emulsion method [23, 24]. The organic solvent in which Cu-oleate or deuterated polystyrene are dissolved is flowed through an aqueous solution at a constant flow rate to generate oil-in-water (O/W) emulsions. Dissolvable materials are suitable for use as targets because it is easy to process the shape and mass produce them in a controllable fabrication process such as the emulsion method [25, 26].

It has been pointed out that experiments involving x-rays and neutrons require different experimental conditions, mainly because inorganic materials such as Cu and organic materials with deuterium are generally incompatible. However, the simultaneous achievement of Cu doping, deuterated polymer, mechanical toughness and chemical robustness during the fabrication process is not so simple. The glow discharge polymer (GDP) method was applied for a Cu-doped deuterated target. In the GDP method deuterated copper (II) acetylacetonate is polymerized on a solid sphere by vapor deposition. However, this method has a problem in that the complicated shape of the

target is difficult to fabricate because it requires a base part to deposit the target. There is no bead target that contains both Cu and deuterium and no simultaneous measurements involving both characteristic x-rays and neutrons. Here we will introduce an example to satisfy these specifications, with chemical and laser plasma characterizations. The target material will open up new ways to investigate progress in FI.

Doping inorganic elements into organic compounds is difficult because the interface between an inorganic and an organic substance generally has a poor affinity; it is also difficult to combine the two substances under conditions with a large interfacial effect, such as a dispersion system of fine particles [27, 28]. The concentration of tracer atoms should be adjustable from 1 to 10 wt% depending on the experimental conditions, since too high a Cu concentration (more than 10 wt%) leads to weak Cu Kα emission due to resonant self-absorption and x-ray measurement will be difficult [28]. In this regard, we report the fabrication of Cu-doped deuterated methyl methacrylate (MMA) and methacrylic acid (MAA) targets (Cu-dMA targets) as novel targets for laser fusion experiments. Cu-dMA is soluble in various solvents, facilitating processing into various shapes, which is difficult for conventional Cu-doped deuterated targets fabricated by the GDP method. The Cu concentration in the Cu-dMA targets is studied using inductively coupled plasma optical emission spectrometry (ICP-OES). The Cu-dMA targets are characterized by simple dissolution tests, differential scanning calorimetry (DSC) and Fourier transform infrared spectroscopy (FTIR). Our results suggest that Cu-dMA targets can be used as targets to provide valuable insights in the IFE experiments.

2. Experiments

2.1. Material fabrication

A schematic diagram of the fabrication process is shown in figure 1. Methyl methacrylate-d_8 (MMA-d_8) monomer was purchased from Cambridge Isotope Laboratories, Inc., yield 98%, stabilized with 10–100 ppm hydroquinone. Methacrylic acid-d_6 (MAA-d_6) monomer was purchased from Central Chemicals Co., Inc., yield 98%, stabilized with hydroquinone. The polymerization inhibitor of MMA-d_8 and MAA-d_6 was removed by washing with Al_2O_3. Azobis(isobutyronitrile) (AIBN) with at least 97% purity was purchased from Kanto Chemical Co., Ltd, and was used as a polymerization initiator. Copper acetate anhydride (Cu-acetate) from Sigma-Aldrich with a purity of 98% was used. MMA-d_8 (452 mg) and MAA-d_6 (31 mg) were stirred with an ultrasonic cleaner (Sharp Manufacturing System Co., Ltd, UT105) in a vial for 5 min. Then Cu-acetate (75.57 mg) was added and stirred for 72 h.
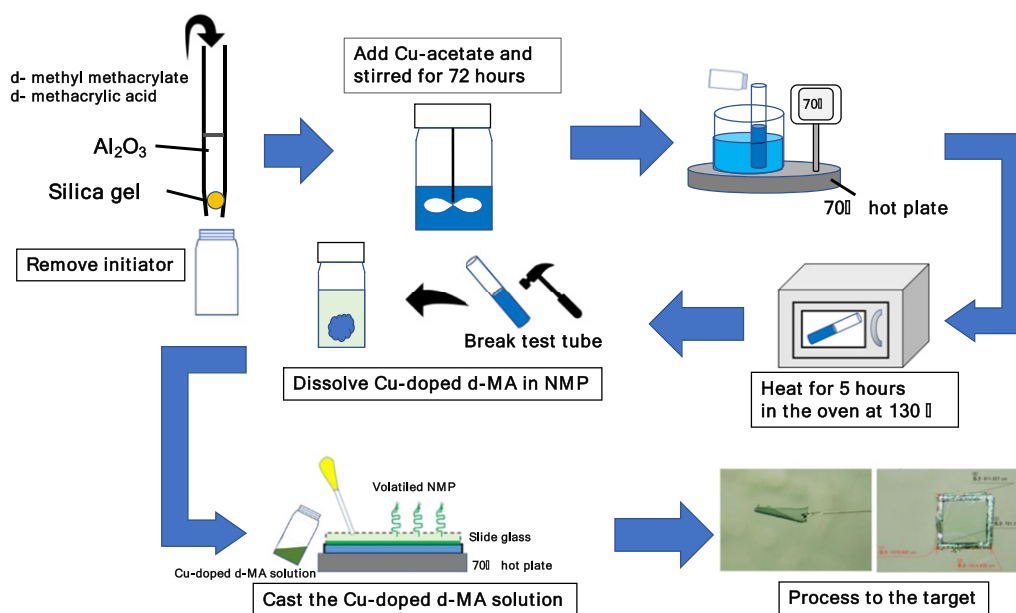
Figure 1. Schematic diagram showing the fabrication process of Cu-doped dMA thin film target.
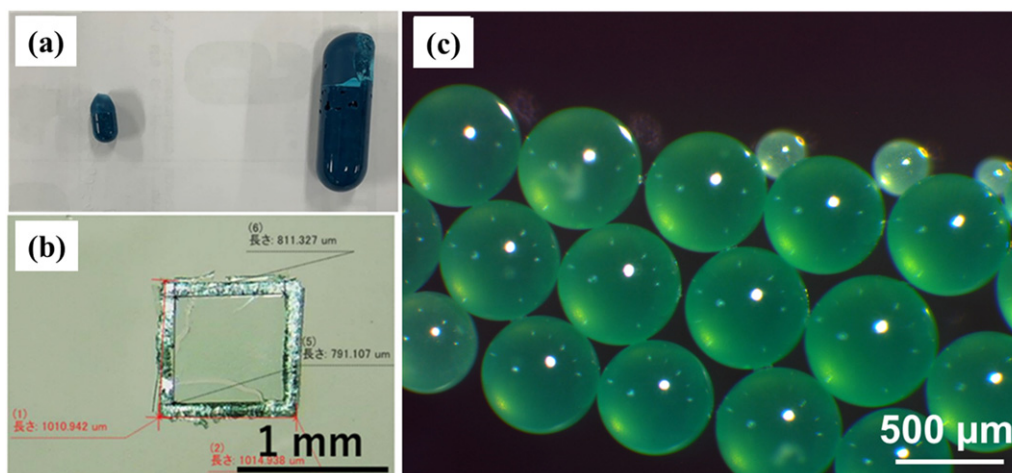

Figure 2. (*a*) Cu-dMA (left) and Cu-hMA (right) samples taken from the oven and the test tube. (*b*) Cu-dMA thin film with a thickness of 10 μm cut to a size of 1 mm × 1 mm. (*c*) Photograph of the Cu-hMA spheres fabricated by dropping the Cu-hMA solution into 10 wt% PVA aqueous solution.

AIBN (0.002 31 mg, 0.5 wt%) was added into the above solution as an initiator and mixed by sonication for 10 min to dissolve. The mixture in the vial was transferred to a test tube and placed in a silicon-oil bath at 70 °C for 11 h in a nitrogen atmosphere for polymerization. The obtained polymer in the test tube was placed in the oven and dried at 130 °C for 5 h to remove unreacted monomers and other ingredients. Finally, 0.18 g Cu-doped deuterated target material based on a MMA/MAA copolymer target (Cu-doped dMA or Cu-dMA) was fabricated. The atomic composite ratio of the sample estimated from the starting materials is H:D:C:O:Cu = 2.4:49.7:32.8:14.3:0.8. To make a film, the Cu-doped dMA target solution was prepared at 2.5 wt% by mixing the plastic samples with *N*-methylpyrrolidone (NMP) (Kishida Chemical Co., Ltd, purity 99.5%) for several days. Then 1.00

ml of solution was spread on a glass slide (size 76 mm × 26 mm, Muto Pure Chemicals Co., Ltd) on a hot plate using a micropipette and heated at 70 °C for 30 min to remove NMP. NMP completely volatilized, and a Cu-doped dMA thin film with a thickness of 10 μm was obtained.

Spherical Cu-hMA (non-deuterated) targets were also fabricated by the emulsion method. A Cu-hMA solution was prepared at 5 wt% by mixing Cu-hMA target material with phenyl acetonitrile (Kishida Chemical Co., Ltd, purity 99.5%). A glass capillary microfluidic device with a 500 μm diameter orifice was employed to generate O/W emulsions, i.e. Cu-hMA droplets in 10 wt% poly(vinyl alcohol) (PVA, Sigma-Aldrich Co., Ltd) aqueous solution [29, 30]. The 500 μm diameter Cu-hMA droplets were produced and subsequently set in a rotary shaker and agitated for 2–3 days to remove organic

Table 1. The contents of reaction mixture for the polymerization.

	Copper acetate (g)	Methyl methacrylate (g)	Methacrylic acid (g)	AIBN (g)
PMMA	None	4.505	None	0.022 83 (0.5 wt%)
hMA-1	None	0.450	0.030	0.002 95 (0.5 wt%)
hMA-2	None	0.450	0.028	0.009 30 (1.5 wt%)
Cu-hMA-1	0.075 59 (4.7 wt%)	0.449	0.032	0.002 90 (0.5 wt%)
Cu-hMA-2	0.075 24 (4.7 wt%)	0.448	0.034	0.009 85 (1.5 wt%)
Cu-hMA-3	0.540 32 (3.5 wt%)	4.501	0.261	0.023 81 (0.5 wt%)
Cu-dMA-1	0.075 57 (4.7 wt%)	0.452	0.031	0.002 31 (0.5 wt%)
Cu-dMA-2	0.046 43 (4.7 wt%)	0.397	0.022	0.009 22 (1.5 wt%)

solvents from the droplets. The emulsion removed from a rotary shaker was dried at room temperature for 1 day, and Cu-hMA spheres were finally obtained. An image of the fabricated Cu-hMA spheres taken with an optical microscope is shown in figure 2.

The starting materials of samples used for characterizations are summarized in table 1.

2.2. Characterization

2.2.1. ICP-OES.
The Cu-dMA-1 targets were characterized using different spectroscopic and calorimetric techniques. Atomic Cu concentration was measured by ICP-OES (PerkinElmer Japan Co., Ltd, Optima 8300). Table 1 shows the sample list with detailed information on each sample characterized by ICP-OES. The samples were initially prepared by putting a Cu-dMA-1 thin film cut into 10 mg to 20 mg pieces in nitric acid (HNO_3, 0.4 cm^3), sulfuric acid (H_2SO_4, 1 cm^3) and perchloric acid ($HClO_4$, 0.1 cm^3) solution and then heated to perfectly dissolve the Cu ions. After heating, Cu salts were obtained and diluted with water to 100 ml. Furthermore, we investigated the change in the amount of Cu doped in the Cu-dMA target material due to the difference in the polymerization kinetics. The Cu-dMA-2, Cu-hMA-1 and Cu-hMA-2 samples, which use different amounts of polymerization initiator, were measured for copper doping in the same way as the Cu-dMA-1 sample.

2.2.2. DSC.
To obtain information on the glass transition temperature (T_g) of the synthesized polymer, the Cu-hMA-1, Cu-dMA-1, hMA-1 and homo PMMA samples were prepared for DSC (Rigaku Co., Ltd, DSC8270). Ten milligrams of the finely crushed thin films were weighed out, and the same amount of Al_2O_3 was used as a reference during measurement. The measurement conditions were as follows: temperature range at temperature rise 20–250 °C, N_2 atmosphere, rate of temperature increase 10 °C min^{-1}. The targets were naturally cooled until their temperature reached room temperature. After cooling, measurements were taken again under the same conditions to reduce the effect on the results of substances adhering to the sample.

2.2.3. FTIR.
The Cu-dMA-1, Cu-hMA-1, hMA-1 and hMA-2 thin films were measured by FTIR. All samples were 10 μm thick.

2.2.4. Dissolution test.
The structure of the synthesized polymer was predicted by a dissolution test in water. For the dissolution test, the Cu-hMA-3 sample was prepared using the method described in section 2.1. The Cu-hMA-3 sample was kept in water for 1 day to confirm whether the Cu had dissolved.

## 3. Results and discussion

3.1. ICP-OES

ICP-OES measurements show that the concentration of atomic Cu doped in the Cu-dMA-1 thin film target prepared in this work was approximately 8.9 wt%. From the weights of Cu-acetate, MMA-d_8 and MAA-d_6 used in the experiment, the theoretical atomic Cu concentration in the thin film was predicted to be approximately 4.7 wt%, but more Cu was doped than expected. However, the result for the Cu-dMA-2 thin film prepared under different conditions was 3.3 wt%, approximately corresponding to the theoretical concentration of 3.5 wt%. The major difference between the Cu-dMA-1 and Cu-dMA-2 thin films was the weight of AIBN used as the polymerization initiator, as shown in table 1. Therefore, two Cu-hMA thin films with 4.7 wt% Cu were additionally prepared with 0.5 and 1.5 wt% AIBN to compare the effects of AIBN concentration. As the result, the Cu-hMA-1 and Cu-hMA-2 thin films contained 5.2 wt% and 4.6 wt% of Cu atoms, respectively. Furthermore, the amount of final product for the Cu-hMA-1 sample was 0.30 g and for the Cu-hMA-2 sample it was 0.20 g, although the amount of monomer and the other preparation conditions were the same. The probable cause of these observed differences is the volatilization of MMA (boiling point 101 °C) during polymerization. Larger amounts of AIBN, which is a polymerization initiator, lead to a rapid polymerization reaction with a lower degree of polymerization, but when the amount of AIBN is as little as 0.5 wt% the polymerization reaction proceeds slowly with a higher degree of polymerization. As the result of this slower reaction process, the unreacted monomer volatilized, resulting in a higher Cu concentration of 8.9 wt% for the Cu-dMA-1 thin film and 5.2 wt% for the Cu-hMA-1 thin film (table 2).

3.2. DSC

The thermal behaviors of the obtained materials are useful for the target fabrication process as well as characterization of the synthesized polymer. The DSC traces of the methacrylic acid (MA) targets and homo-PMMA are shown

Table 2. Results of atomic Cu concentration measured by ICP-OES for each sample.

	Cu-acetate (g)	AIBN (g)	Estimates (Cu wt%)	Results (Cu wt%)
Cu-hMA-1	0.075 59	0.002 90 (0.5 wt%)	4.7	5.2
Cu-hMA-2	0.075 24	0.009 85 (1.5 wt%)	4.7	4.6
Cu-dMA-1	0.075 57	0.002 31 (0.5 wt%)	4.7	8.9
Cu-dMA-2	0.046 43	0.009 22 (1.5 wt%)	3.5	3.3
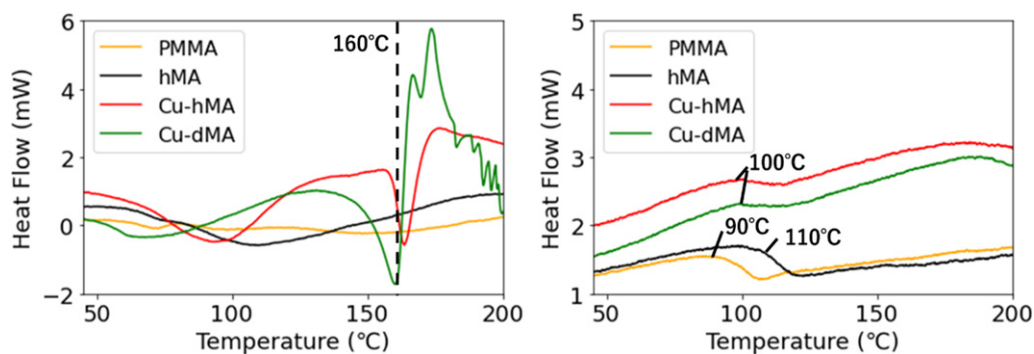
Figure 3. The DSC trace of the MA targets and PMMA at the first (left) and second (right) temperature rise.
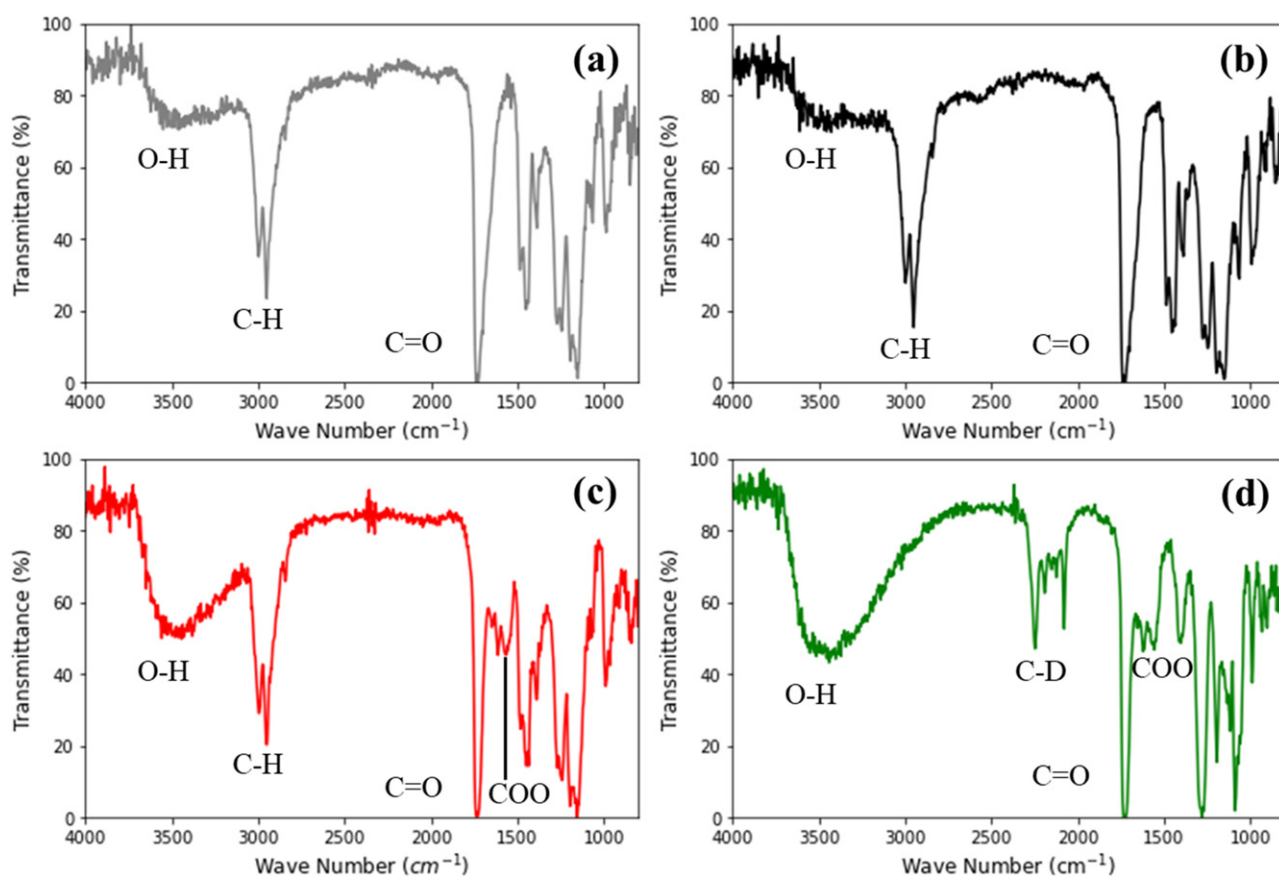
Figure 4. FTIR spectra of (*a*) hMA-1, (*b*) hMA-2, (*c*) Cu-hMA-1 and (*d*) Cu-dMA-1 thin films.

in figure 3. In the first DSC measurement, an endothermic peak was observed around 160 °C in the case of Cu-hMA-1 and Cu-dMA-1, which corresponds to the boiling point of methacrylic acid. From the DSC trace of PMMA, and the results of the dissolution test described later, it is considered that the addition of Cu-acetate inhibited the polymerization

Figure 5. Photograph of the dissolved Cu-hMA-3 sample in distilled water after 1 day.
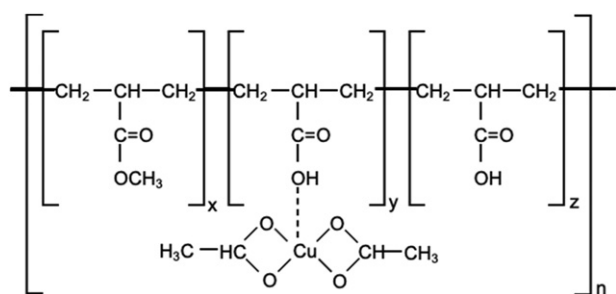

Figure 6. Coordination position of Cu-acetate to poly-MMA-co-MAA as predicted from the FTIR spectra.

reaction and reduced the molecular weight. In the second DSC measurement, the homo-polymers show a shift in DSC trace at approximately 90 °C, which corresponds to the T_{g} of PMMA [27, 31]. MA also shows a glass transition at approximately 110 °C near the T_{g} of PMMA, and Cu-hMA-1 and Cu-dMA-1 show a change at approximately 100 °C. Therefore, hMA-1, Cu-hMA-1 and Cu-dMA-1 samples are expected to be polymers.

3.3. FTIR

Figure 4 shows the FTIR spectra of the Cu-dMA-1, Cu-hMA-1, hMA-1 and hMA-2 thin films. From the comparison of the

FTIR spectra of the hMA-1 thin film in figure 4(*a*) and the hMA-2 thin film in figure 4(*b*), it was found that there was almost no change in the structure of the copolymer due to the difference in the amount of AIBN. From the comparison of the FTIR spectra of the Cu-hMA thin film in figure 4(*c*) and the hMA-1 thin film in figure 4(*d*), the peak at 3500 cm^{-1} derived from the OH bond of MAA became larger and the peak at 1590 cm^{-1} from the carboxyl group of Cu-acetate appeared due to the addition of Cu-acetate [32–36]. Thus, it can be deduced that the Cu atom in the Cu-hMA-1 sample does not exist alone but is coordinated to the polymer as Cu-acetate. In addition, Cu-acetate is likely to coordinate to the hydroxy group of MAA in the polymer due to the increase in peaks derived from the O–H bond after doping with Cu-acetate. Since there is no significant difference in the FTIR spectra of the Cu-hMA-1 thin film and hMA-1 thin film other than the peaks mentioned above, we conclude that the Cu-hMA-1 polymer also has a similar structure to poly(MMA-co-MAA) of hMA-1 and hMA-2. Finally, by comparing Cu-dMA-1 (figure 4(*d*)) and Cu-hMA-1 (figure 4(*c*)), the peaks from the C–H bond in MMA and MAA are shifted due to deuteration.

3.4. Chemical characterization from the viewpoint of the target material

After the Cu-hMA3 had been kept in water for a day, it was confirmed that the distilled water in the vial had turned pale blue (figure 5), suggesting that the Cu component of the Cu-hMA-3 sample had dissolved. In the plastic sample fabricated in this work, if the Cu atoms are bonded to MMA or MAA monomers by the polymerization reaction and are contained in the chain structure of the polymer, it is unlikely that the Cu component will dissolve in water. Therefore, for both Cu-hMA and Cu-dMA it is predicted that the Cu atoms used in the materials are coordinated to any part of the polymer as a ligand. It is reasonable that highly coordinated Cu compounds will dissolve in water following a previous report [37, 38].

The DSC results clarify the existence of volatile components, for example unreacted monomer and dissociated volatile ligands of acetic acid, in the first heating process, and the components would not be seen in the second heating due to their removal. In the present case the possible exchange of the Cu ligand is from acetic acid to polymethacrylate, and gives free acetic acid (boiling point 120 °C). The DSC result did not show such an endothermic peat at 120 °C, indicating no exchange of the ligand of Cu-acetate. Next, FTIR spectra showed a peak at 1590 cm^{-1} owing to the C=O bond with Cu coordination, and this should not be Cu polymethacrylate because this must give free acetic acid which is not observed in the DSC. Therefore the peak at 1590 cm^{-1} must be characterized as the Cu-acetate in the starting material. Furthermore, the FTIR spectra show the existence of the polymer backbone of polymethacrylate and PMMA as shown in figure 6 [39]. From the ICP-OES results, the concentration of Cu and the amount of methacrylic acid is comparable in the samples.
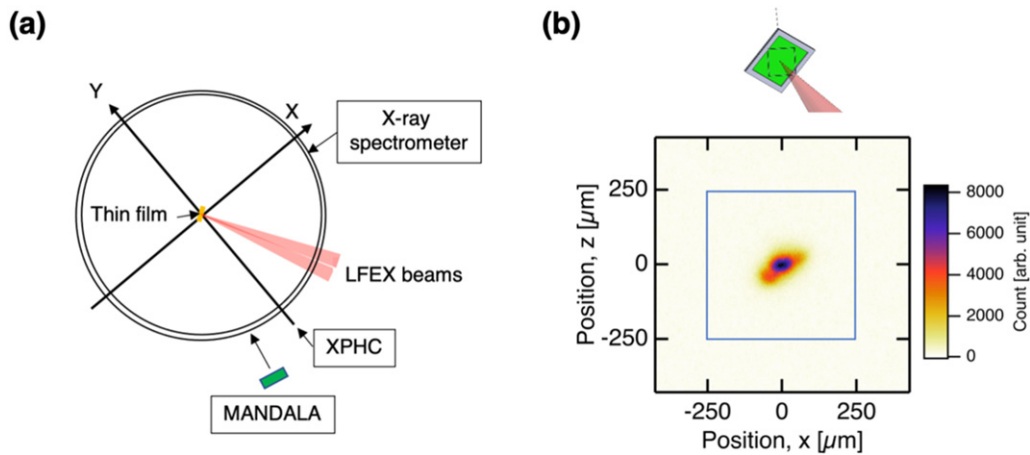
Figure 7. (*a*) Illumination layout and diagnostics (shot number L4236). (*b*) X-ray pinhole image from the film surface: (top) the target and laser illumination view from the x-ray pinhole camera port with a 500 μm square box; (bottom) x-ray image on the target surface.
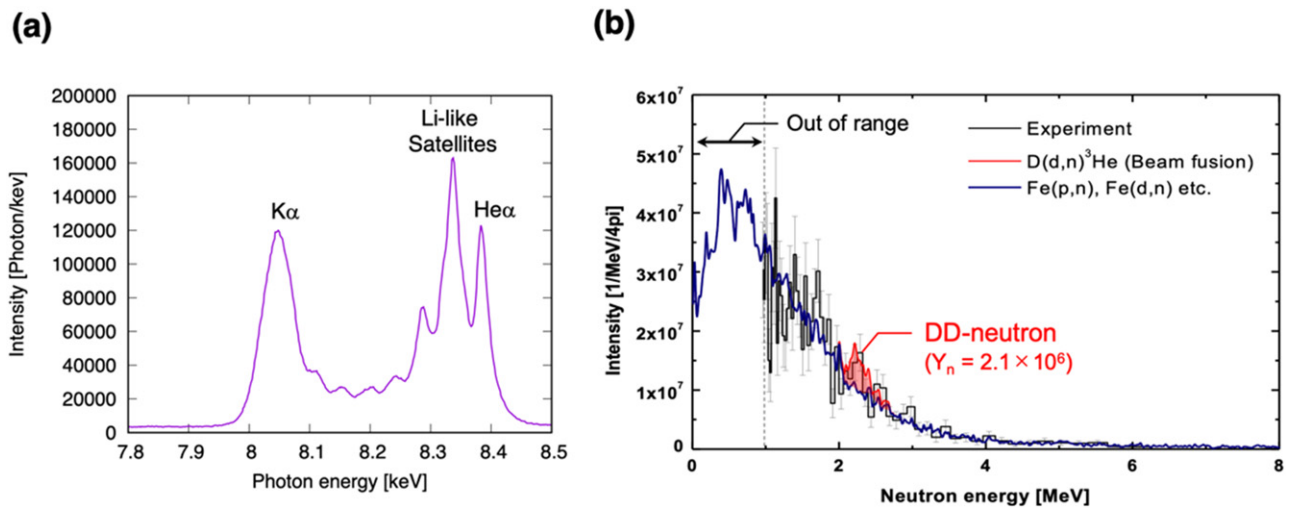

Figure 8. (*a*) X-ray spectrum emitted from the film target measured by the HOPG spectrometer. (*b*) Neutron spectrum obtained by time-of-flight measurement, showing multiple components associated with beam fusion (D(d,n)^{3}He reaction), Fe(d,n) and Fe(p,n) reactions.

4. Demonstration of laser irradiation on the Cu-dMA thin film target

The fabricated Cu-dMA thin film target was illuminated by a petawatt laser for fast ignition experiments (LFEX) to demonstrate the generation of characteristic x-rays and fusion neutrons simultaneously. The Cu-dMA target material fabricated in this study was processed into a thin film with a thickness of 10 μm and a size of 1 mm $\times$ 1 mm, then fixed to an aluminum frame to create the Cu-dMA thin film target, as shown in figure 2(*b*). Figure 7(*a*) shows the layout for laser illumination into this thin film and the diagnostics. The laser LFEX system consists of four beams of a kJ-class Nd:glass chirped pulse amplification system [40]. In this experiment, by using off-axial parabolic mirrors, four beams were focused into the center of the chamber, where the film was placed, with a total energy of 248 J and pulse duration at full width half maximum (FWHM) of 1.3 ps. The focal intensity was 5×10^{18} W cm^{-2}, evaluated from the focal spot diameter of 70 μm FWHM measured from an CW alignment laser, resulting in a normalized

field amplitude a_0 of 2.0. The diagnostics comprised an x-ray pinhole camera [41] and x-ray spectrometer utilizing highly oriented pyrolytic graphite (HOPG) as a diffractor for the x-ray detection [42] and a multichannel time-of-flight neutron spectrometer (MANDALA) for neutron detection [43]. Figure 7(*b*) shows the x-ray pinhole image on the target surface. This x-ray image indicates that four beams are focused into the target center with a focal spot size of 77 μm FWHM, comparable to that measured by the alignment laser. This result confirmed that four beams were successfully focused into the target center to achieve relativistic laser–matter interactions.

The Cu-dMA target can contribute to the measurement of both characteristic x-rays and neutrons simultaneously. Characteristic x-ray generation from the thin film was confirmed from the HPOG x-ray spectrometer. Figure 8(*a*) shows the x-ray spectrum from the film. The peak of 8.048 keV indicates the Cu Kα line, and peaks around 8.35 keV indicate the Cu Heα line and Li-like satellite lines. Electron temperature can be evaluated from the intensity ratio of the Heα line to the

Li-like lines. Neutron generation from the deuteron–deuteron fusion reaction was confirmed by the multi-channel neutron spectrometer. Figure 8(*b*) shows the neutron spectrum obtained by time-of-flight measurement using the multi-channel scintillation detector MANDALA. Neutrons with energies around 2.45 MeV (red line in figure 8(*b*)) with yield of 2.1×10^6 neutrons for 4π sr are produced primarily via beam fusion [44], which is caused by the bombardment of bulk deuterium by $\sim$100 keV deuterons accelerated on the front surface of the film. This neutron yield is comparable with the previous experiments [45], in which a deuterated polystyrene film without Cu doping was illuminated by a Nd-glass CPA laser, taking account of on-target laser differences. Deuteron-induced neutron production also occurs in the target chamber wall and diagnostic instruments around the target. Those neutrons are produced via Fe(d,n) and Al(d,n) reactions, resulting in a broad spectral range from sub-MeV to multi-MeV (blue line in figure 8(*b*)).

5. Conclusion

In conclusion, a Cu-doped deuterated target thin film was fabricated in this work. We succeeded in deuterating the target and doping the target with Cu. Copper acetic anhydride, MMA and methacrylic acid were used as the monomers. In addition, the amount of doped Cu could be increased to 8.9 wt% by controlling the amount of AIBN. We succeeded in developing solid microspheres using Cu-hMA by the emulsion method. This target can be shaped more easily and freely than the conventional Cu-doped deuterated target fabricated by the GDP method. Finally, we confirmed that the fabricated Cu-dMA thin film target can be used for laser experiments to measure characteristic x-rays and fusion neutrons simultaneously. Based on these simultaneous measurements, we can improve the accuracy of quantitative values of the high-energy-density state leading to realization of IFE.

Acknowledgments

ORCID iDs

Keisuke Shigemori https://orcid.org/0000-0002-3978-8427
Marilou Cadatal-Raduban https://orcid.org/0000-0001-9641-132X
Keiji Nagai https://orcid.org/0000-0002-7641-562X
Shinsuke Fujioka https://orcid.org/0000-0001-8406-1772
Hiroshi Sawada https://orcid.org/0000-0002-7972-9894
Yoshitaka Mori https://orcid.org/0000-0001-7754-9171
Kohei Yamanoi https://orcid.org/0000-0003-4492-4099

References

[1] Basov N.G., Gus'kov S.Y. and Feokistov L.P. 1992 Thermonuclear gain of ICF targets with direct heating of ignitor *J. Russ. Laser Res.* **13** 396

[2] Tabak M., Hammer J., Glinsky M.E., Kruer W.L., Wilks S.C., Woodworth J., Campbell E.M., Perry M.D. and Mason R.J. 1994 Ignition and high gain with ultrapowerful lasers *Phys. Plasmas* **1** 1626

[3] Kodama R. *et al* 2001 Fast heating of ultrahigh-density plasma as a step towards laser fusion ignition *Nature* **412** 798

[4] Kodama R. *et al* 2002 Fast heating scalable to laser fusion ignition *Nature* **418** 933

[5] Kitagawa Y. *et al* 2005 Petawatt-laser direct heating of uniformly imploded deuterated-polystyrene shell target *Phys. Rev.* E **71** 016403

[6] Theobald W. *et al* 2011 Initial cone-in-shell fast-ignition experiments on OMEGA *Phys. Plasmas* **18** 056305

[7] Shiraga H., Nagatomo H., Theobald W., Solodov A.A. and Tabak M. 2014 Fast ignition integrated experiments and high-gain point design *Nucl. Fusion* **54** 054005

[8] Kitagawa Y. *et al* 2015 Direct heating of a laser-imploded core by ultraintense laser-driven ions *Phys. Rev. Lett.* **114** 195002

[9] Jarrott L.C. *et al* 2016 Visualizing fast electron energy transport into laser-compressed high-density fast-ignition targets *Nat. Phys.* **12** 499

[10] Fujioka S. *et al* 2016 Fast ignition realization experiment with high-contrast kilo-joule peta-watt LFEX laser and strong external magnetic field *Phys. Plasmas* **23** 056308

[11] Mori Y. *et al* 2016 Fast heating of imploded core with counter-beam configuration *Phys. Rev. Lett.* **117** 055001

[12] Mori Y. *et al* 2017 Fast heating of fuel assembled in a spherical deuterated polystyrene shell target by counter-irradiating tailored laser pulses delivered by a HAMA 1 Hz ICF driver *Nucl. Fusion* **57** 116031

[13] Sakata S. *et al* 2018 Magnetized fast isochoric laser heating for efficient creation of ultra-high-energy-density states *Nat. Commun.* **9** 3937

[14] Gong T. *et al* 2019 Direct observation of imploded core heating via fast electrons with super-penetration scheme *Nat. Commun.* **10** 5614

[15] Matsuo K. *et al* 2020 Petapascal pressure driven by fast isochoric heating with a multipicosecond intense laser pulse *Phys. Rev. Lett.* **124** 035001

[16] Merkuliev Y.A. *et al* 2006 Laser targets from new solid materials with high concentration of hydrogen isotopes for neutron generation *J. Phys. IV France* **133** 887–90

[17] Borisenko N.G. *et al* 2013 Laser study into and explanation of the direct–indirect target concept *EPJ Web Conf.* **59** 03014

[18] Borisenko N.G., Dorogotovtsev V.M., Gromov A.I., Guskov S.Y., Merkul'ev Y.A., Markushkin Y.E., Chirin N.A., Shikov. A.K. and Petrunin V.F. 2017 Laser targets of beryllium deuteride *Fusion Technol.* **38** 161–5

[19] Pastukhov A.V. *et al* 2022 Fabrication of hollow poly(alpha-methylstyrene) shells for inertial confinement fusion targets *J. Appl. Polym. Sci.* **139** e52997

[20] Sawada H. *et al* 2011 Monochromatic imaging of 8.0 keV Cu Kα emission induced by energetic electrons generated at OMEGA EP *IEEE Trans. Plasma Sci.* **39** 2816

[21] Habara H., Honda S., Katayama M., Sakagami H., Nagai K. and Tanaka K.A. 2016 Efficient energy absorption of intense ps-laser pulse into nanowire target *Phys. Plasmas* **23** 063105

[22] Kaneyasu Y., Nagai K., Cadatal-Raduban M., Golovin D., Shokita S., Yogo A., Jitsuno T., Norimatsu T. and Yamanoi K. 2021 Fabrication of disk-shaped, deuterated resorcinol/formaldehyde foam target for laser-plasma experiments *High Power Laser Sci. Eng.* **9** e31

[23] Iwasa Y. *et al* 2017 Cu-oleate microspheres fabricated by emulsion method as novel targets for fast ignition laser fusion experiments *Fusion Eng. Des.* **125** 89

[24] Iwasa Y.K., Yamanoi Y., Kaneyasu T. and Norimatsu T. 2018 Controlled generation of double emulsions for laser fusion target fabrication using a glass capillary microfluidic device *Fusion Sci. Technol.* **73** 258

[25] Nagai K., Nakajima M., Norimatsu T.Y., Izawa T. and Yamanaka T. 2000 Solvent removal during curing process of highly spheric and monodispersed-sized polystyrene capsules from density-matched emulsions composed of water and benzene/1,2-dichloroethane *J. Polym. Sci.* A **38** 3412

[26] Nagai K. *et al* 2009 Fabrication of aerogel capsule, bromine-doped capsule, and modified gold cone in modified target for the Fast Ignition Realization Experiment (FIREX) Project *Nucl. Fusion* **49** 095028

[27] Furusawa K. and Anzai C. 1987 Preparation of composite fine particles by heterocoagulation *Colloid Polym. Sci.* **265** 882

[28] Furusawa K. and Anzai C. 1992 Heterocoagulation behaviour of polymer latices with spherical silica *Colloids Surf.* **63** 103

[29] Utada A.S., Lorenceau E., Link D.R., Kaplan P.D., Stone H.A. and Weitz D.A. 2005 Monodisperse double emulsions generated from a microcapillary device *Science* **308** 537

[30] Uchida Y., Takanishi Y. and Yamamoto J. 2013 Controlled fabrication and photonic structure of cholesteric liquid crystalline shells *Adv. Mater.* **25** 3234

[31] Kuo S.W., Kao H.-C. and Chang F.-C. 2003 Thermal behavior and specific interaction in high glass transition temperature PMMA copolymer *Polymer* **44** 6873

[32] Higqy E.S.M. *et al* 1986 Some physical and spectroscopic studies on methyl methacrylate-copper acrylate bulk copolymers *Acta Polym.* **37** 606–9

[33] Rufino E.S. and Monteiro E.E.C. 2003 Infrared study on methyl methacrylate-methacrylic acid copolymers and their sodium salts *Polymer* **44** 7189

[34] Zhang Z., Zhang M., Luo L., Yang X., Hu Y., Zhang H. and Yao S. 2010 Synthesis and application of core–shell complex-imprinted polymer for the solid-phase extraction of melamine from dairy products *J. Sep. Sci.* **33** 2854

[35] Kuroda Y., Sasano A. and Kubo M. 1966 Infrared spectra of urea complexes of copper(II)n-alkanoates *Bull. Chem. Soc. Japan* **39** 1002

[36] Ibrahim M. *et al* 2005 Density functional theory and FTIR spectroscopic study of carboxyl group *Indian J. Pure Appl. Phys.* **43** 911

[37] Yamaoka K. and Masujima T. 1979 Spectroscopic and equilibrium dialysis studies of the poly(acrylic acid)-Cu(II) complex in the pH range 3.5-7 *Bull. Chem. Soc. Japan* **52** 1819

[38] Yamashita Y., Komatsu T. and Nakagawa T. 1979 Study of metal-polycarboxylate complexes employing ion-selective electrodes: II. Stability constants of copper(II) complexes with poly(acrylic acid) and poly(methacrylic acid) *Bull. Chem. Soc. Japan* **52** 30

[39] AkutaKishi S.T. and Nagai T. 1972 Electrophoretic deposition of poly-MMA-MAA and poly-MMA *Electrochemistry* **40** 810

[40] Miyanaga N. *et al* 2006 10-kJ PW laser for the FIREX-I program *J. Phys. IV France* **133** 81

[41] Miura E. *et al* 2020 Verification of fast heating of core plasmas produced by counter-illumination of implosion lasers *High Energy Density Phys.* **37** 100890

[42] Zastrau U. *et al* 2012 Focal aberrations of large-aperture Hopg von-Hàmos x-ray spectrometers *J. Instrum.* **7** P09015

[43] Abe Y. *et al* 2014 Development of multichannel time-of-flight neutron spectrometer for the fast ignition experiment *Plasma Fusion Res.* **9** 4404110

[44] Abe Y. *et al* 2020 Monte Carlo particle collision model for qualitative analysis of neutron energy spectra from anisotropic inertial confinement fusion *High Energy Density Phys.* **36** 100803

[45] Izumi N. *et al* 2002 Observation of neutron spectrum produced by fast deuterons via ultraintense laser plasma interactions *Phys. Rev.* E **65** 036413